Available online at www.sciencedirect.com
ScienceDirect
Journal of Colloid and Interface Science 311 (2007) 507–513
JOURNAL OF Colloid and Interface Science
www.elsevier.com/locate/jcis

Preparation and self-assembly of carboxylic acid-functionalized silica

Yanqing An [a,b,c], Miao Chen [a,*], Qunji Xue [a], Weimin Liu [a]

[a] State Key Laboratory of Solid Lubrication, Lanzhou Institute of Chemical Physics, Chinese Academy of Sciences, Lanzhou 730000, China
[b] Laboratory of Special Functional Materials, Henan University, Kaifeng 475001, China
[c] Graduate University of the Chinese Academy of Sciences, Beijing 100049, China

Received 6 September 2006; accepted 26 February 2007

Available online 3 March 2007

Abstract

A simple method for the fabrication of silica nanoparticle film based on the covalent-bonding interaction between carboxylic acid-functionalized silica nanoparticles (SiO_2–COOH) and amino-terminated silicon wafer was developed. Prior to assembly, silica nanoparticles with an average diameter 80 nm were prepared using the Stöber method, amino-functionalized silica nanoparticles (SiO_2–NH_2) were prepared by a silanization with 3-aminopropyltriethoxysilane (APTES), while carboxylic acid-functionalized silica nanoparticles (SiO_2–COOH) were prepared by a ring opening linker elongation reaction of the amine functions with succinic anhydride, at the same time, amino-terminated silicon wafer (Si–NH_2) was obtained by self-assembling 3-aminopropyltriethoxysilane, then one layer relative close-packed carboxylic acid-functionalized silica nanoparticles (SiO_2–COOH) was arranged on silicon wafer through amidation reaction under DCC coupling agent.

Keywords: Surface functionalization; Covalent assembly; Amidation; Carboxylic acid-functionalized silica nanoparticles

1. Introduction

The organization of nanoparticles in film form is important for applications [1,2]. Self-assembly of nanoparticle by the colloidal on suitable supports is one of the interesting techniques currently being investigated for realizing such structure because of the colloid size controllability and monodispersity [3]. Nanostructure based on silica nanoparticles has found extensively applications in areas like optoelectronic devices [4,5], MEMS device [6], photonic crystal [7,8], chemical/biological sensor [9,10].

Various techniques such as electrostatic assembly [10,11], colloidal epitaxy [12,13], convective self-assembly [14,15], physisorption mediated by surface tension [16], and application of an external electric field [17,18] have been employed to direct the assembly of nanoparticles on surface. However, there existed weak adsorption between these nanoparticles and the substrate [19]. Recently, covalent interactions have been utilized to bind the nanoparticles to a substrate, and it is considered necessary for nanoparticles and the substrate to have active groups [20–22]. Amine group and carboxyl group have brought attention due to their better activity.

Surface modification is usually used to obtain reactive group on silica nanoparticles, most of the recent literatures concerning surface modification are based on surface grafting organosilanes onto silica [23,24], and amine, vinyl, dendrime, and pyridine especially amine group which has been applied extensively in biomedical. However a very limited member of articles describes the modification of carboxyl group to silica nanoparticle surface. Carboxyl groups on silica surface were obtained by trichlorocyanoethylsilane (TCES) [19], polymer [25] and succinic anhydride [26,27] through different methods, especially succinic anhydride converts amino groups into carboxyl groups easily without higher temperature or additional catalyst [28,29].

Here, we describe a method to assemble nanoparticles to the silicon directly by amidation between amine group of silicon surface and carboxyl group of the modified silica nanoparticles. The silica nanoparticles derivated from the conversion of amino-functionalized into carboxylic acid-functionalized by a ring opening linker elongation reaction of the amine functions with succinic anhydride, and silicon

* Corresponding author. Fax: +86 931 8277088.
E-mail address: miaochen@lzb.ac.cn (M. Chen).

0021-9797/$ – see front matter
doi:10.1016/j.jcis.2007.02.084

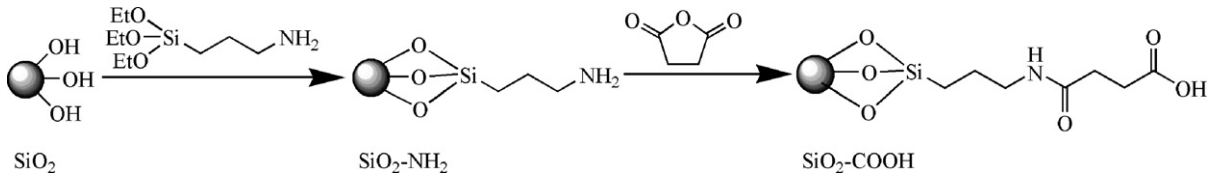

Scheme 1. Process of preparing the carboxylic acid-functionalized silica nanoparticles.

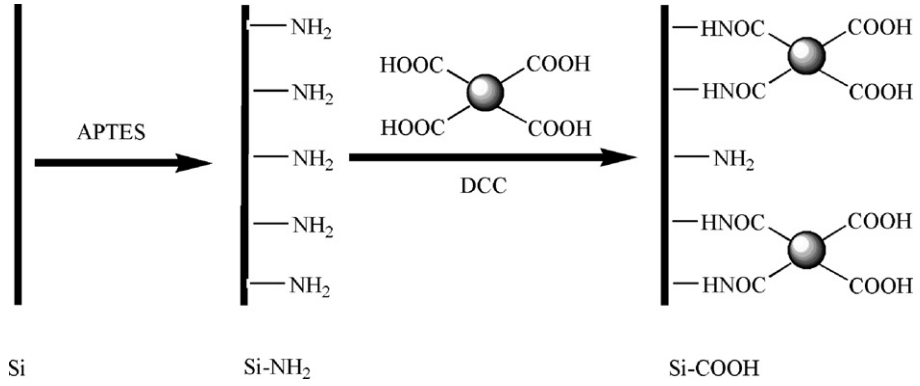

Scheme 2. Process of carboxylic acid-functionalized silica nanoparticles self-assembly on silicon substrate.

surface was amino-terminated through self-assembling with 3-aminopropyltriethoxysilane. The surface was terminated with carboxyl group, which is active to further react with relevant reagents.

2. Experimental

2.1. Chemicals

3-Aminopropyltriethoxysilane (APTES, 99%) was obtained from Acros, tetraethoxysilane (TEOS), ammonium hydroxide, succinic anhydride, *N*,*N*-dimethylformamide (DMF), *N*,*N*-dicyclohexylcarbondiimide (DCC), anhydrous ethanol, and acetone were analytical grade without further purification. Double distilled water was used.

2.2. Preparation of amino-functionalized silica nanoparticles

Amino-functionalized silica nanoparticles (SiO_2–NH_2) were prepared using the modified Stöber method [28–30]. Briefly, 4 ml of tetraethoxysilane (TEOS) was added to a mixture of 3.3 ml ammonium hydroxide and 47 ml of ethanol with stirring, the reaction was continued 24 h; the resulting silica colloidal dispersion was functionalized with APTES by quickly added 0.3 ml of APTES with a vigorously stirring. The mixture was stirred overnight. The nanoparticle was purified by centrifugation and redispersion in ethanol. Above procedure was repeated three times. Meanwhile, bare silica nanoparticles (SiO_2) obtained under the same condition without addition of APTES.

2.3. Preparation of carboxylic acid-functionalized silica nanoparticles

A dispersion of SiO_2–NH_2 obtained in DMF (20 ml) was added dropwise to a flask containing 20 ml of 0.1 M succide anhydride in DMF. The mixture was stirred for 24 h, the resulting silica nanoparticles with carboxylic-function groups at their surface (SiO_2–COOH) were cleaned as described above. DMF was used as the washing medium.

The procedure of preparing the carboxylic acid-functionalized silica nanoparticles are summarized in Scheme 1.

2.4. Carboxylic-functionalized silica nanoparticles (SiO_2–COOH) self-assembly film on silicon wafer

Scheme 2 illustrates the procedure to assembly carboxylic-functionalized silica nanoparticles to silicon wafer surface. Silicon wafer was cleaned in piranha solution ($H_2SO_4/H_2O_2 = 7{:}3$ v/v) for 3 h at 90 °C, and then rinsed with water and acetone thoroughly. The cleaned substrates were placed into the APTES solution of 5.0×10^{-3} M in a mixture solvent of acetone and ultra-pure water (v/v = 5:1), and kept for 3 h, followed by rinsing with acetone and ethanol, the target monolayer of APTES was thus formed on the hydroxylated silicon surface (Si–NH_2).

A dispersion of SiO_2–COOH in DMF (10 ml) was sonicated for 10 min. DCC was added to this solution as a condensing agent. After 3 h, APTES modified silicon (Si–NH_2) was then immersed in this solution for 24 h at room temperature. After having been rinsed with DMF and water, carboxylic-functionalized silica nanoparticle (SiO_2–COOH) self-assembly film formed on silicon wafer, and the silicon surface was terminated with carboxyl group (Si–COOH).

2.5. Characterization

The diameter and morphology of nanoparticles were investigated by JEM-1200EX transmission electron micrographs (TEM). DLS measurements and zeta potential of the nanoparticle were performed with a Zetasizer nano-ZS ZEN3600 (Malvern instruments Ltd., US). The compositions of nanopar-

ticles were determined by a thermorgravimetric analysis (PE7-TGA) and PHI-5700 X-ray photoelectron spectroscopy (XPS). The thickness of the films was measured on a Gaertner L116-E ellipsometer, static contact angles were measured with a Kyowa contact-angle meter, and atomic force microscopy (AFM) images were obtained by using a nanoscope IIIa (Veeco, Digital Instruments).

3. Result and discussion

3.1. Particle characterization

The relatively monodisperse silica nanoparticles were generated by the Stöber method. 3-Aminopropyltriethoxysilane (APTES) was used to introduce priming amine groups to the particles by a silanization. The carboxylic acid group was obtained by a ring opening linker elongation reaction of the amine group with succinic anhydride. The conversion was qualitatively tested by salicylaldehyde [28,31]. Upon addition of salicylaldehyde, SiO_2–NH_2 turned yellow immediately, indicating the presence of amino groups, whereas SiO_2–COOH was hardly observed yellow even after 24 h. This is a clear indication that most of the amino groups have reacted.

3.1.1. TEM and size analysis

The modification of surface was accompanied by change of surface charge of silica nanoparticle, which was confirmed by zeta potential measurements, and change to both particle size and polydispersity (PD) (Table 1, Fig. 1). The SiO_2–NH_2 nanoparticle aggregated in water for it has the point of zero charge while the pH value between 7 and 8. In our experiments, although the SiO_2–NH_2 was washed three times after reaction, ammonium hydroxide cannot be removing completely. The solution showed alkalescence and a low negative zeta potential at

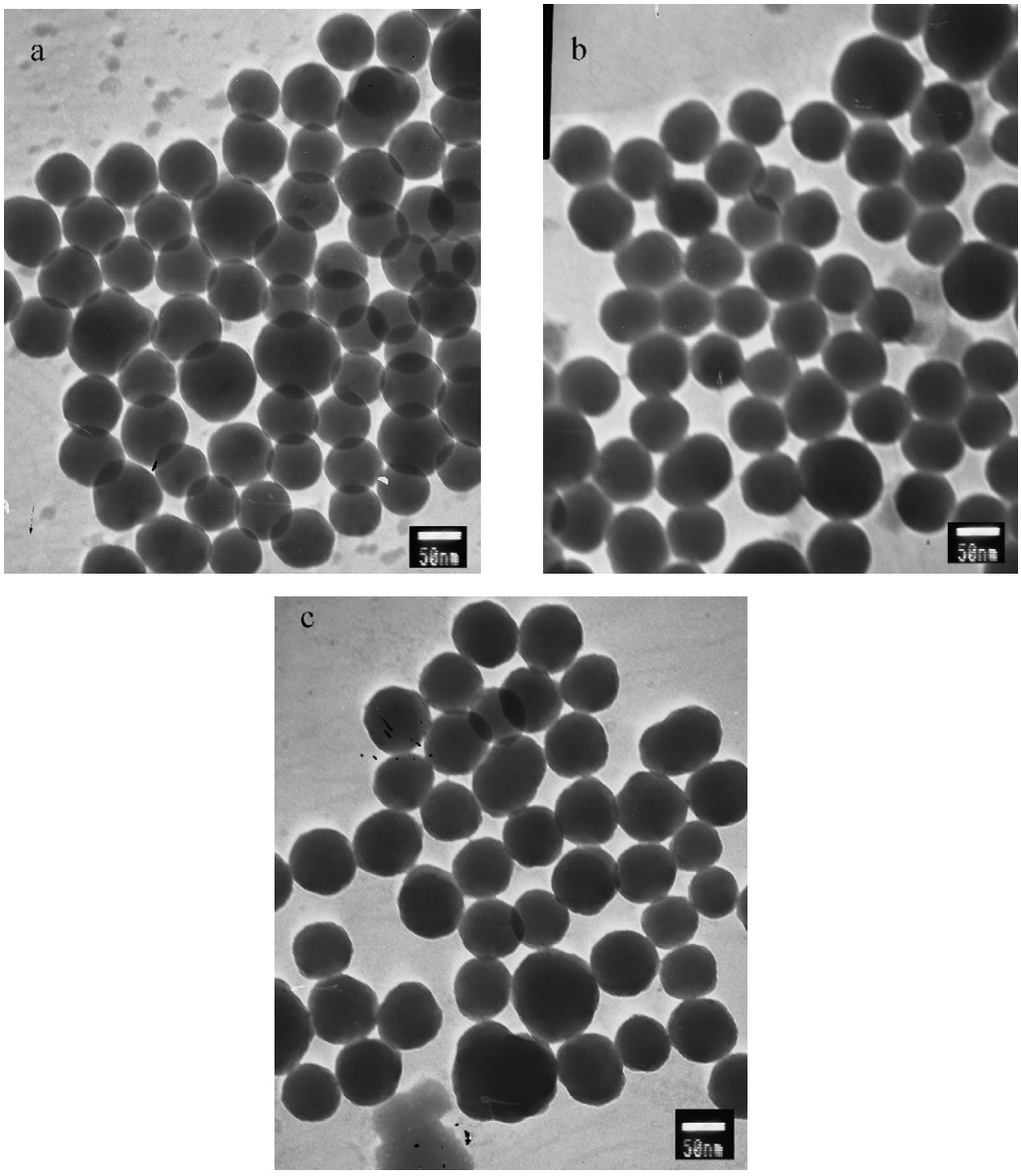

Fig. 1. TEM photographs of SiO_2 nanoparticles (a), SiO_2–NH_2 nanoparticles (b) and SiO_2–COOH nanoparticles (c).

about −10.15 mV, so SiO_2–NH_2 aggregated in a short time, which agrees with the result by Schiestel [29]. It is found from Fig. 1 that SiO_2, SiO_2–NH_2 and SiO_2–COOH are of similar size because the additional organic group does not increase the volume of nanoparticle obviously. The single particle of diameter was between 70 and 100 nm, while the average particle size determined by Zetasizer was about 139 nm. The difference obtained from DLS and TEM imaging resulted from the different underlying principle of the applied methods [32]. For TEM, preparation of the samples required dilution of the solution of nanoparticles, dry samples are used that may not reflect the particle distribution present in solution, whereas for DLS, measurements are collected in solution, and the size of the particles in solution were affected by the pH, solvent and other factors of solution.

Table 1
Characteristics of silica nanoparticles

	Zeta potential (mV)	Mean diameter (nm)	PDI
SiO_2	−35.33	139.4	0.077
SiO_2–NH_2	−10.15	Aggregate	
SiO_2–COOH	−42.21	135.5	0.030

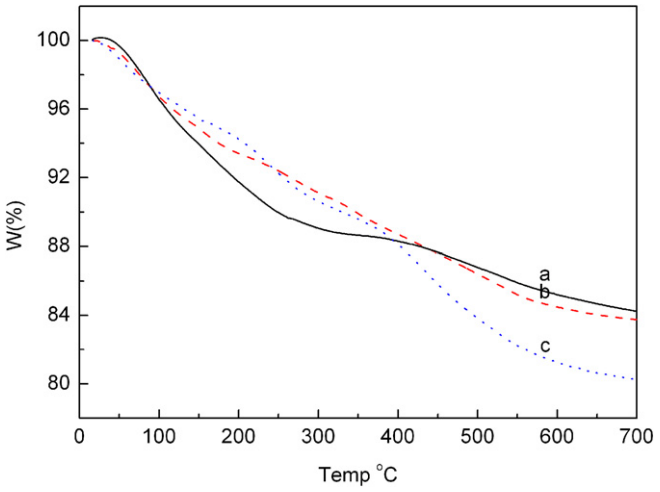

Fig. 2. Thermogravimetic analyses of SiO_2 nanoparticles (a), SiO_2–NH_2 nanoparticles (b) and SiO_2–COOH nanoparticles (c).

3.1.2. TGA and XPS analysis

The organic content of the surface modified silica nanoparticles assessed by TGA. Fig. 2 shows the respective weight loss curves of SiO_2, SiO_2–NH_2 and SiO_2–COOH. The loss weight of SiO_2 is relatively low due to removal of absorbed water and adventitious hydrocarbon contamination. Fig. 2b shows a higher mass loss than that of SiO_2 which indicated that APTES modified onto the SiO_2. The largest loss weight among them was indicated in Fig. 2c. Compare the curves of b with c, we can see that the organic content of the nanoparticle increases from 16.5 to 19.7%, which indicated further derivatization reaction of SiO_2–NH_2 was carried out by succide anhydride.

Investigation of the chemical composition of the nanoparticle surfaces was carried out by XPS. The XPS survey scans of SiO_2, SiO_2–NH_2 and SiO_2–COOH are presented in Fig. 3. The apparent surface compositions of silica nanoparticles are reported in Table 2. The presence of C1s peak at 284.6 eV in Fig. 3a is due to contamination of the bare silica during the XPS spectrometer operation, while N1s peak is detected in Figs. 3b and 3c in addition to Si, O and C; the atom percent of N is 4.41% and 3.84%, respectively. Both SiO_2–NH_2 and SiO_2–COOH contain nitrogen elements from APTES. The changes of contents of Si, O and C element between the SiO_2–NH_2 and SiO_2–COOH is quite small. The high resolution spectra of N element were analyzed and showed in Fig. 4. In Fig. 4a, the N element for SiO_2 does not appear, after treated with APTES, the N1s spectrum (Fig. 4b) for SiO_2–NH_2 reveals two components: one is corresponded to free amino group at 399.1 eV with a con-

Table 2
Apparent surface compositions (at%) of silica nanoparticles as determined by XPS

	C (at%)	N (at%)	O (at%)	Si (at%)
SiO_2	22.83	0	55.88	21.29
SiO_2–NH_2	30.37	4.41	43.80	21.41
SiO_2–COOH	36.99	3.84	41.81	17.35

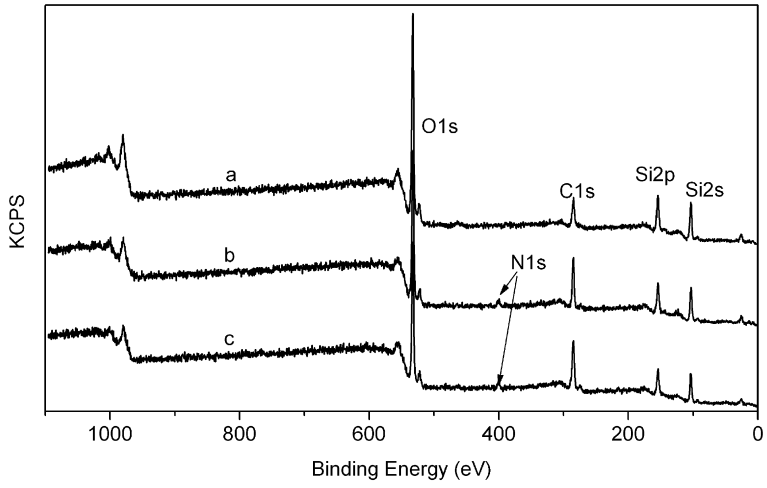

Fig. 3. XPS survey scans of SiO_2 nanoparticles (a), SiO_2–NH_2 nanoparticles (b) and SiO_2–COOH nanoparticles (c).

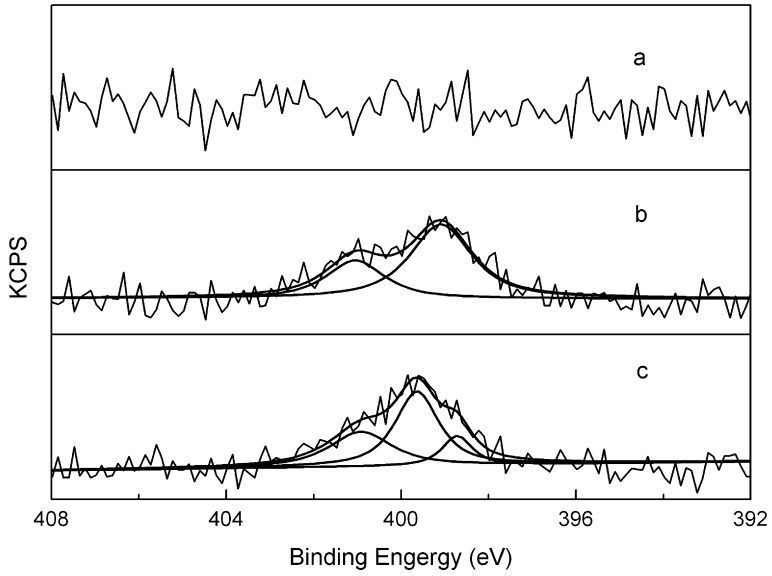

Fig. 4. XPS N1s spectra for SiO_2 nanoparticles (a), SiO_2–NH_2 nanoparticles (b) and SiO_2–COOH nanoparticles (c).

Table 3
Contact angle and thickness for the silicon and the modified silicon surface

	θ (measurement)	θ (reference)	Thickness (nm)
Si (after piranha)	5	5	2
Si–NH_2	47	48	0.8
Si–COOH	15	27	70

tent about 67.5%, and the other peak at 401.1 eV (32.5%) may be due to some interactions between the amino groups undergo H-bonding with each other or with substrate hydroxyls [33]. At the ring opening linker elongation reaction step, the N1s spectrum for SiO_2–COOH could be deconvoluted into three peaks. The amide group presented in the N1s spectrum at 399.6 eV was about 51.4%, the content of free amino group (at 398.7 eV) decrease to 14%, and the content of the other peak at 400.9 eV was 34.6%, which was almost similar to the sample of SiO_2–NH_2. This suggested that the N element of amide group came from the reaction of the amine free group with the succinic anhydride.

3.2. Characterizations of self-assembly film

3.2.1. Contact angle and thickness measurement

Contact angle measurement is an effective way to reflect the variation of solid-surface chemical composition. The contact angle for water on the pretreated silicon surface and the self-assembled films thereon are shown in Table 3. At least five replicate measurements were carried out for each specimen, and the measurement error was below 2°. The obtained contact angles for the pretreated silicon surface and APTES modified silicon surface is about 5° and 47°, respectively, which are all in agreement with the previously reported value [34,35]. When SiO_2–COOH nanoparticles was assembled on the silicon wafer, the contact angle is about 15°, because that –COOH is more hydrophilic compared with –NH_2, according to the work of Toworfe [36], in which the contact angle of –COOH terminated self-assembly monolayers (SAMs) modified silicon wafer about 27°. The difference results from the surface roughness, the RMS of the nanoparticle film in this work is about 24 nm, while the RMS of the –COOH terminated self-assembly monolayers (SAMs) is only a few nanometer, according the Wenzel's law, the contact angle will decrease with increased roughness of a hydrophilic surface [37].

Table 3 shows the thickness change from the bare silicon wafer to SiO_2–COOH nanoparticle assembled film. Five replicate measurements were carried out for each specimen. The oxide coating thickness on the silicon wafer after piranha solution treatment (prior to salinization) was measured as 2 nm by ellipsometry. After the formation of silane layers on the surface, the thickness of the APTES SAMs was determined to be approximately 0.8 nm, similar to the data of elsewhere papers [34] the thickness mentioned above was recorded to an accuracy of ±0.3 nm. After SiO_2–COOH film was formed, the film thickness greatly increases to 70 nm which has an error of 4 nm.

3.2.2. AFM characterization

Typical AFM images of self-assembled SiO_2–COOH on APTES modified silicon obtained using the tapping mode in air were shown in Fig. 5. Fig. 5a shows the image of SiO_2–COOH self-assembled film in the presence of DCC. Fig. 5c shows the image of SiO_2–COOH self-assembled film without DCC coupling agent. It is easy to identify the bright quasi-spherical space with SiO_2–COOH, while the background in a darker gray scale, corresponds to the APTES modified silicon. Compared Fig. 5a with Fig. 5c, only small number of silica nanoparticles were adsorbed without DCC even for more then 72 h. The nanoparticles density was almost invariable from 6 to 72 h, only a few nanoparticles attached on the silicon surface which might caused by electrostatic interactions or hydrogen bond. The density of silica nanoparticle on amine-modified surface was increased intensively until 24 h by using DCC and slowly a close-packed nanoparticle film was formed,

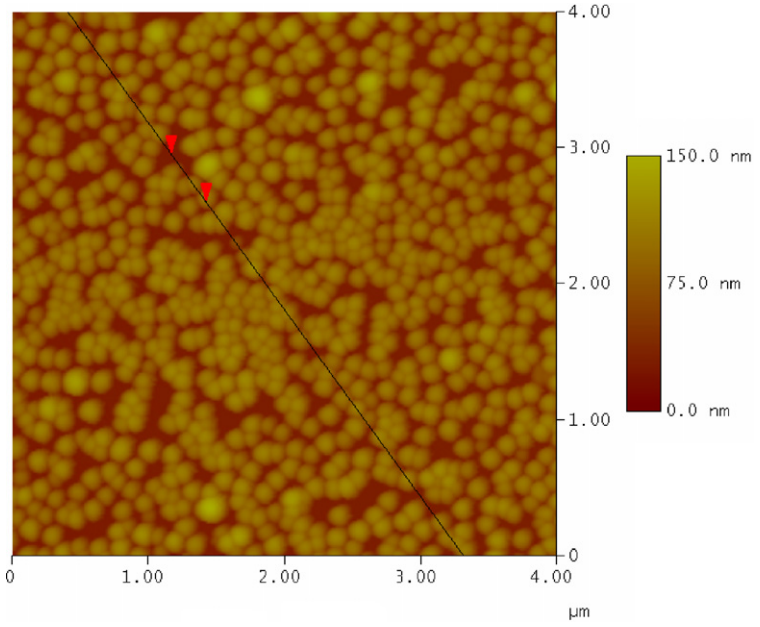

(a)

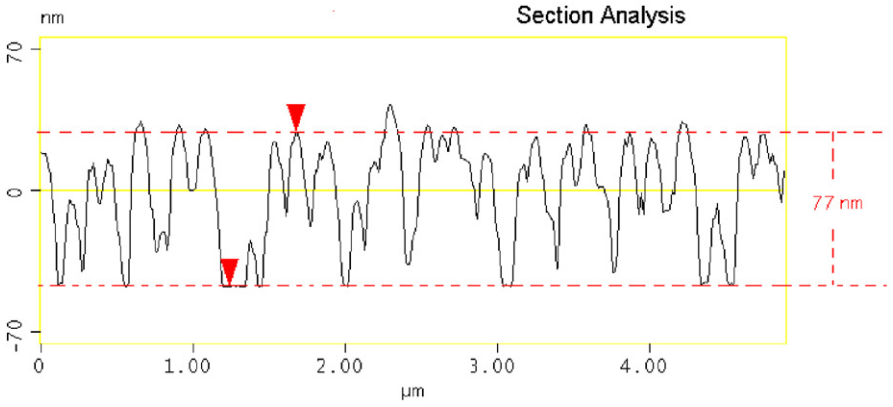

(b)

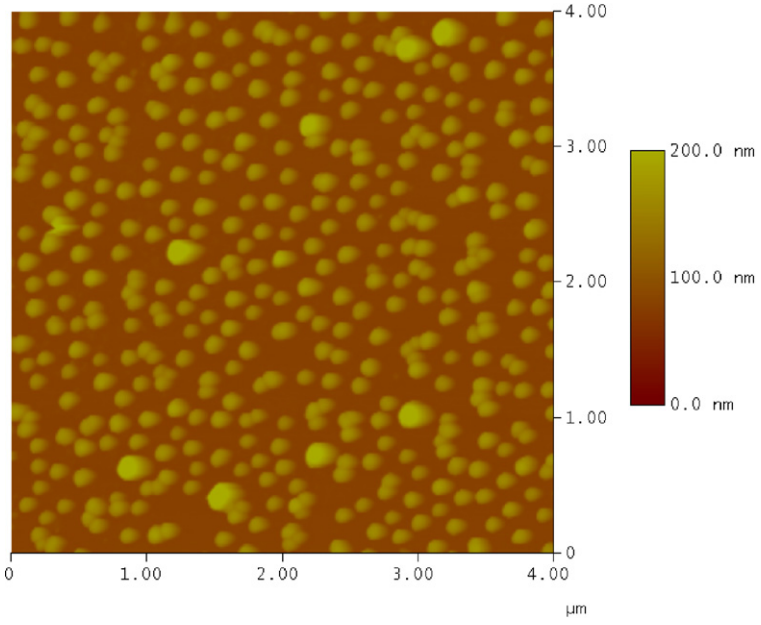

(c)

Fig. 5. AFM image of SiO_2–COOH nanoparticles assembled film in DCC (a), the corresponding section analysis (b) and AFM image of SiO_2–COOH nanoparticles assembled film without DCC (c).

which similar to Park's work [38]. That means the covalent bond between a carboxylic group functionalized silica nanoparticles and an amine-modified silicon wafer was formed by using DCC. Fig. 5b shows corresponding typical height profile measured in the linear regions of Fig. 5a. By analyzing the profile, the film has an average height of about 77 nm, a value similar to the SiO_2–COOH diameter, which indicated the film was composed of one layer SiO_2–COOH. Compared with the thickness of film by ellipsometry, we can conclude that the nanoparticles assembly via covalent bond is an efficient way to reach close-packed relatively one layer SiO_2–COOH nanoparticles film.

4. Conclusions

Amino- and carboxyl-functional groups were covalently coupled to the surface of silica nanoparticles easily, then SiO_2–COOH nanoparticles self-assembled film were formed on silicon by amidation successfully. One layer relative close-packed SiO_2–COOH nanoparticles were arranged on silicon wafer. Compared to the existing methods, it is evident that covalently bonding of carboxyl groups of silica nanoparticle to aminosilane groups on silicon is an effective method of bonding silica nanoparticles. It is envisaged that functionalized nanoparticle assemblies will serve as a platform for further assembly of relevant information such as nanoparticle, biomolecule, fluorescence indicator and so on.

Acknowledgments

Supports from Natural Science Foundation of China (Grant No. 20473106), the 973 project (Grant No. 2003CB716200) of Chinese Ministry of Science and Technology and the Innovation Group foundation (No. 50421502) are gratefully acknowledged.

References

[1] A.N. Shipway, E. Katz, I. Willner, Chem. Phys. Chem. 1 (2000) 18.
[2] Y. Xia, B. Gates, Y. Yin, Y. Lu, Adv. Mater. 12 (2000) 693.
[3] H. Hattori, Adv. Mater. 13 (2001) 51.
[4] M. Sastry, Curr. Sci. 78 (2000) 1089.
[5] F. Hua, J. Shi, Y. Lvov, T. Cui, Nanotechnology 14 (2003) 453.
[6] M. Zou, L. Cai, H. Wang, Tribol. Lett. 20 (2005) 43.
[7] O. Toader, S. John, Science 292 (2001) 1133.
[8] E. Vekris, V. Kitaev, G. von Freymann, D.D. Perovic, J.S. Aitchison, G.A. Ozin, Adv. Mater. 17 (2005) 1269.
[9] E. Rampazzo, E. Brasola, S. Marcuz, F. Mancin, P. Tecilla, U. Tonellato, J. Mater. Chem. 15 (2005) 2687.
[10] J.H. Fendler, Chem. Mater. 8 (1996) 1616.
[11] H. Ow, D.R. Larson, M. Srivastava, B.A. Baird, W.W. Webb, Nano Lett. 5 (2005) 113.
[12] B.F. Lyles, M.S. Terrot, P.T. Hammond, A.P. Gast, Langmuir 20 (2004) 3028.
[13] W. Lee, A. Chan, M.A. Bevan, J.A. Lewis, P.V. Braun, Langmuir 20 (2004) 5262.
[14] B.G. Prevo, O.D. Velev, Langmuir 20 (2004) 2099.
[15] B.G. Prevo, Y. Hwang, O.D. Velev, Chem. Mater. 17 (2005) 3642.
[16] F. Lenzmann, K. Li, A.H. Kitai, H.D.H. Stover, Chem. Mater. 6 (1994) 156.
[17] G. Cao, J. Phys. Chem. B 108 (2004) 19921.
[18] B.B. Yellen, O. Hovorka, G. Friedman, Proc. Natl. Acad. Sci. USA 102 (2005) 8860.
[19] Y. Masuda, W.S. Seo, K. Koumoto, Thin Solid Films 382 (2001) 183.
[20] Y. Ma, L. Qian, H. Huang, X. Yang, J. Colloid Interface Sci. 295 (2006) 583.
[21] Y. Fu, H. Xu, S. Bai, D. Qiu, J. Sun, Z. Wang, X. Zhang, Macromol. Rapid Commun. 23 (2002) 256.
[22] J.C. Riboh, A.J. Haes, A.D. McFarland, C.R. Yonzon, R.P. Van Duyne, J. Phys. Chem. B 107 (2003) 1772.
[23] G. Deng, M.A. Markowitz, P.R. Kust, B.P. Gaber, Mater. Sci. Eng. C 11 (2000) 165.
[24] A.S. Maria Chong, X.S. Zhao, J. Phys. Chem. B 107 (2003) 12650.
[25] K. Yoshinaga, F. Nakashima, T. Nishi, Colloid Polym. Sci. 277 (1999) 136.
[26] H. Kim, Y.S. Chung, H. Paik, M. Kim, J. Suh, Bioorg. Med. Chem. Lett. 12 (2002) 2663.
[27] L. Levy, Y. Sahoo, K. Kim, E.J. Bergey, P.N. Prasad, Chem. Mater. 14 (2002) 3715.
[28] V. Mahalingam, S. Onclin, M. Peter, B.J. Ravoo, J. Huskens, D.B. Reinhoudt, Langmuir 20 (2004) 11756.
[29] T. Schiestel, H. Brunner, G.E.M. Tovar, J. Nanosci. Nanotech. 4 (2004) 504.
[30] W. Stöber, A. Fink, E.J. Bohn, J. Colloid Interface Sci. 26 (1968) 62.
[31] A. van Blaaderen, A. Vrij, J. Colloid Interface Sci. 156 (1993) 1.
[32] W. Lesniak, X. Shi, A. Bielinska, K. Janczak, K.S.J.R. Baker Jr., L.P. Balogh, Mater. Res. Soc. Symp. Proc. 845 (2005) AA5.37.1.
[33] F. Zhanf, M.P. Srinivasan, Langmuir 20 (2004) 2309.
[34] S. Ren, S. Yang, S. Yang, Y. Zhao, Langmuir 19 (2003) 2763.
[35] Z.Q. Wei, C. Wang, C.F. Zhu, C.Q. Zhou, B. Xu, C.L. Bai, Surf. Sci. 459 (2000) 401.
[36] G.K. Toworfe, R.J. Composto, I.M. Shapiro, P. Ducheyne, Biomaterials 27 (2006) 631.
[37] H.M. Shang, Y. Wang, K. Takahashi, G.Z. Cao, D. Li, Y. Xia, J. Mater. Sci. Lett. 40 (2005) 3587.
[38] J.Y. Park, H.W. Lee, Colloids Surf. A 257–258 (2005) 133.